Valve Opening Characteristics – Iteration 1

Anders Hedegaard Hansen
E-mail: AHH@et.aau.dk

1 SUMMERY

First iteration off valve opening algorithms are in this “report” compared. In section 4 it is seen that the energy production is equal for the “old” algorithm(A2-RHH) and the “new” A3. Further significant reduction of the pressure oscillation are seen in situation for which the algorithms are fitted, however, close to no pressure change are seen in situations for which the algorithm are not fitted.
This is a combination of the paper from DFP15 and measurements done thereafter for energy comparison.

2 METHOD

At the instant of a force shift the pressure in at least one cylinder chamber is changed by shifting the connection from one pressure line to another, cf. Fig. 3. This is done by closing the current connection and subsequently opening the new connection. The opening characteristic of the valve to the new connection has significant influence on how the pressure will develop in the cylinder chamber. Four algorithms for the valve opening profile are proposed, which have been implement on a physical test setup and the results compared. In this work the closing of the former connection is disregarded, and hence set to follow a ramp.

2.1 Valve opening algorithms

In [8] the authors propose four flow reference algorithms determining the required valve flow to perform a given pressure shift. These algorithms were theoretically derived and compared utilising simulation models. The algorithms, however, only discussed the required flow through the valve and not how the valve is controlled to give this flow with the time varying pressure difference across. The valve opening algorithms are hence based on the work in [8], where the flow algorithms were developed to perform a given pressure trajectory in the cylinder chamber.

The modelled based flow algorithms from [8] are here briefly introduced and linked to the valve opening algorithms in this paper. The model structure constituting the bases for the flow algorithms utilised in the current work is a simple lumped parameter model of a cylinder chamber and the connecting hose and connected valves, see Fig. 5.

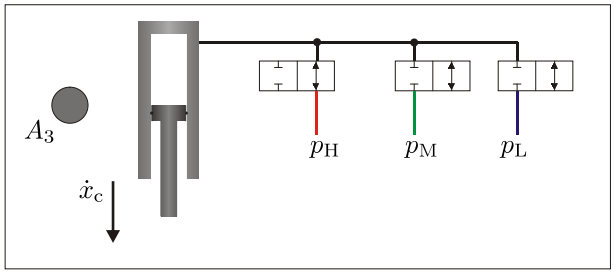

Fig. 5: Model illustration of cylinder chamber three and connecting valves.

For the simple flow algorithms test in the current work the hose dynamic is not included in the model based flow algorithms. Hence the model on which the flow algorithms are based is simply a continuity equation.

$$Q_3 = \dot{x}_c A_3 + \frac{V_3(x_c)+V_{Hose}}{\beta_{eff}} \dot{p}_3 \quad (1)$$

In [8] the required valve flow into the hose was then based on eq. (1) and a reference pressure trajectory. Cleary the smoothness of the pressure trajectory influence the smoothness of the required valve flow as the pressure gradient directly appears in eq (1). When calculating the required flow the piston velocity $\dot{x}_c$ and the piston position x_c is assumed constant during the pressure shift.

In the current paper the required reference flow, $\Delta Q(t)$, is linked to a valve opening via the orifice equation and assuming that the chamber pressure follows the reference trajectory.

$$A_V(t) = \frac{K_V}{\sqrt{\Delta p_V(t)}} \Delta Q(t) \quad (2)$$

With $A_V(t)$ being the valve opening area for the valve with valve coefficient K_V. The pressure drop across the valve is $\Delta p_V(t)$ which is preset by the pressure trajectory.

One should note that assuming constant piston velocity, chamber volume and that the pressure trajectory is followed yield a feedforward algorithm, hence, stability problems will not occur. The piston position, velocity and chamber pressure must be measured at the initiation of the pressure shift only. As the displacement flow due to piston movement may either assist or oppose this is must be accounted for. This is done by including the sign of the piston area by the working direction and multiplying the sign of the pressure changes:

$$\Delta Q(t) = \dot{x}_c A_3 \frac{\Delta p}{|\Delta p|} + \frac{V_3(x_c)+V_{Hose}}{\beta_{eff}} \dot{p}_3 \quad (3)$$

2.1.1 Algorithm 1 - Linear valve opening

A linear opening characteristic is chosen as the standard bench mark opening characteristics. Here the opening area is hence given as:

$$A_V(t) = \frac{A_{V.max}}{T_{Shift}} t \quad (4)$$

Where $A_{v.max}$ is the maximal valve opening area and T_{shift} is the time duration for the valve opening action. Note that is valve opening algorithm do not utilise current piston position and velocity as input contrary to the later.

2.1.2 Algorithm 2 - Linear pressure gradient

The second algorithm is based on the flow algorithm C1 from [8] and was initially proposed in [3] by Hansen et al. A flow reference giving a linear pressure change in the chamber is utilised. The valve opening area reference is calculated assuming that the pressure drop across the valve is linear decreasing according to the linear pressure change in the cylinder chamber and therefore only utilise a one point initial pressure measurement. Hence, the valve reference is given as:

$$A_V(t) = \frac{K_V}{\sqrt{\Delta p_V(t)}} \Delta Q(t) \tag{5}$$

$$\Delta Q(t) = \dot{x}_c(t_0) A_c \frac{\Delta p}{|\Delta p|} + \frac{V_c}{\beta} \frac{|\Delta p|}{T_{shift}} \tag{6}$$

$$\Delta p_V(t) = |\Delta p| \left(1 - \frac{1}{T_{shift}} t\right) \tag{7}$$

Where the pressure change required is Δp and $\dot{x}_c(t_0)$ is the piston velocity at the start, t_0, of the pressure shift. A_c and V_c is the piston area and the cylinder chamber volume respectively. The pressure drop across the valve is $\Delta p_V(t)$ and K_V is the valve flow coefficient. As seen in Eq. (6) the flow reference consists of two terms the displacement flow, which is due to piston movement, and the compressibility flow. Note the flow reference is constant during the full shifting period and the valve pressure drop is linear decreasing from Δp to zero over the full shifting time. The nature of the flow reference, pressure reference and the valve opening reference is given in Fig. 6.

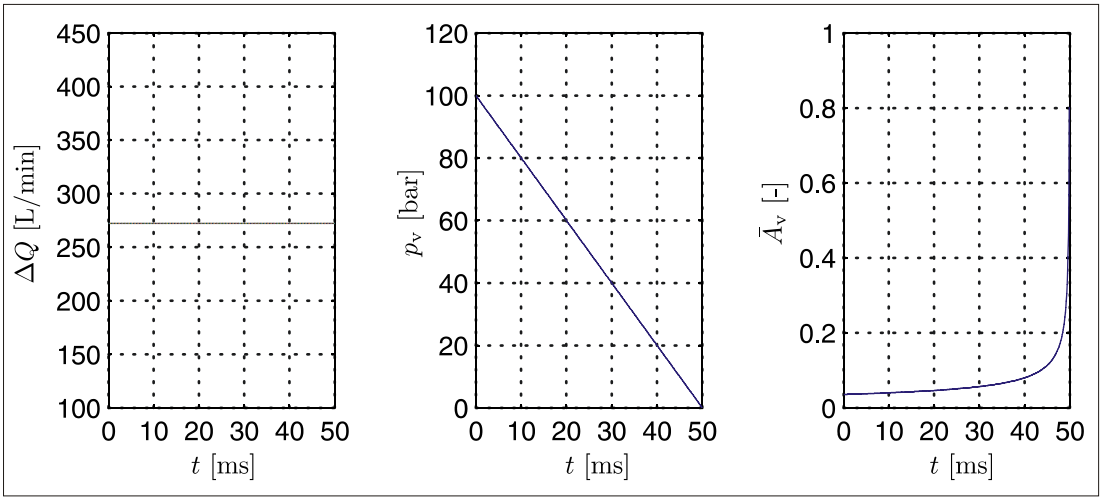

Fig. 6: Illustration of valve opening algorithm 2.

2.1.3 Algorithm 3 - Smooth pressure trajectory (Third order polynomial)

A third order polynomial is proposed as pressure trajectory, where the compression flow reference may be set to zero at the ends of the shifting period. As for the former algorithm the displacement flow is included in the flow reference. The valve opening reference is given as:

$$A_V(t) = \frac{K_V}{\sqrt{\Delta p_V(t)}} \Delta Q(t) \tag{8}$$

$$\Delta Q(t) = \dot{x}_c(t_0) A_c \frac{\Delta p}{|\Delta p|} + \frac{V_c}{\beta} |\Delta p| \left(-\frac{6}{{T_{shift}}^3} t^2 + \frac{6}{{T_{shift}}^2} t \right) \tag{9}$$

$$\Delta p_V(t) = |\Delta p| \left(1 + \frac{2}{{T_{shift}}^3} t^3 - \frac{3}{{T_{shift}}^2} t^2 \right) \tag{10}$$

Note that both the flow reference and the assumed pressure drop is time dependent. The nature of the flow reference, pressure reference and the valve opening reference is given in Fig. 7.

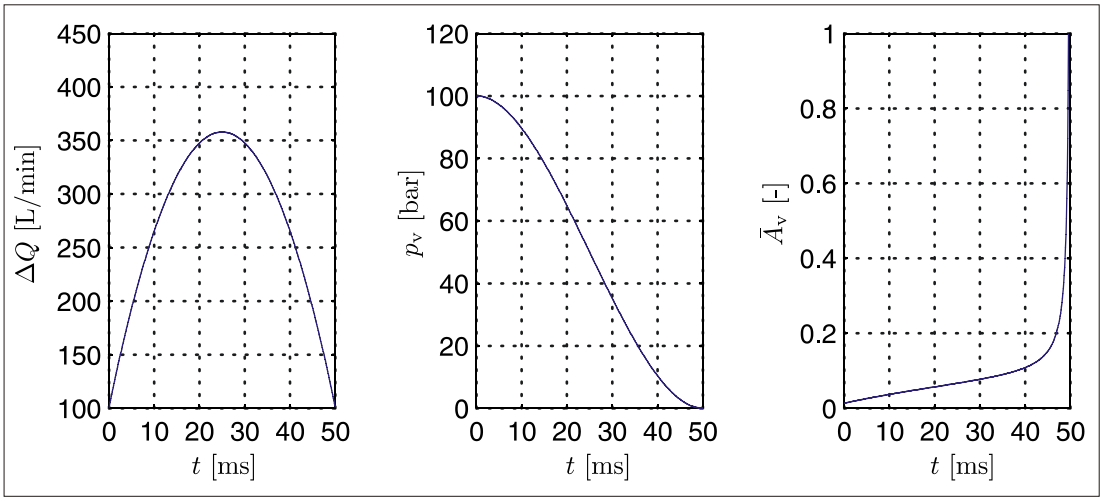

Fig. 7: Illustration of valve opening algorithm 3.

From the figure one may see that the displacement flow in this example is approximately 100L/min.

2.1.4 Algorithm 4 - Smooth pressure trajectory (Fifth order polynomial)

To ensure smooth changes in the pressure gradient a fifth order polynomial is utilised to describe the cylinder pressure reference, such that the derivative of the pressure gradient may be set to zero at both ends of the shifting period. Hence, the compression flow at the ends of the shifting period is zero. Once again the displacement flow is added in the reference flow equation. Hence, the valve opening reference is given as:

$$A_V(t) = \frac{K_V}{\sqrt{p_V(t)}} \Delta Q(t) \tag{11}$$

$$\Delta Q(t) = \dot{x}_c(t_0) A_c \frac{\Delta p}{|\Delta p|} + \frac{V_c}{\beta} |\Delta p| \left(\frac{30}{{T_{shift}}^5} t^4 - \frac{60}{{T_{shift}}^4} t^3 + \frac{30}{{T_{shift}}^3} t^2 \right) \tag{12}$$

$$p_V(t) = |\Delta p| \left(1 - \frac{6}{{T_{shift}}^5} t^5 + \frac{15}{{T_{shift}}^4} t^4 - \frac{10}{{T_{shift}}^3} t^3 \right) \tag{13}$$

Like for algorithm 3 both the assumed pressure drop and the flow reference is time dependent. Compared to the third order polynomial the extension is here that the initial and final pressure gradient is zero, which impose that the valve area is changed more smooth at beginning and end, which comes at the expense of higher peak flows.

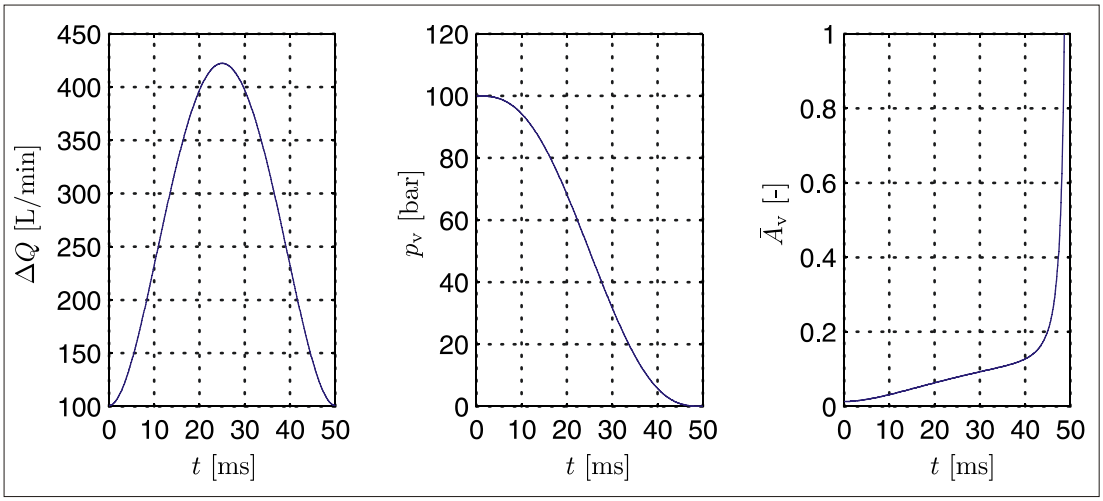

Fig. 8: Illustration of valve opening algorithm 4.

2.2 Test conditions

The implemented algorithms are tested under similar conditions by moving the test cylinder piston with constant velocity and doing the pressure shifts at preset positions hereby ensuring that the chamber volume and volume gradient are equal. The piston velocity and position reference is seen in Fig. 10. The dashed red lines in the position plot indicate where pressure shifts are performed.

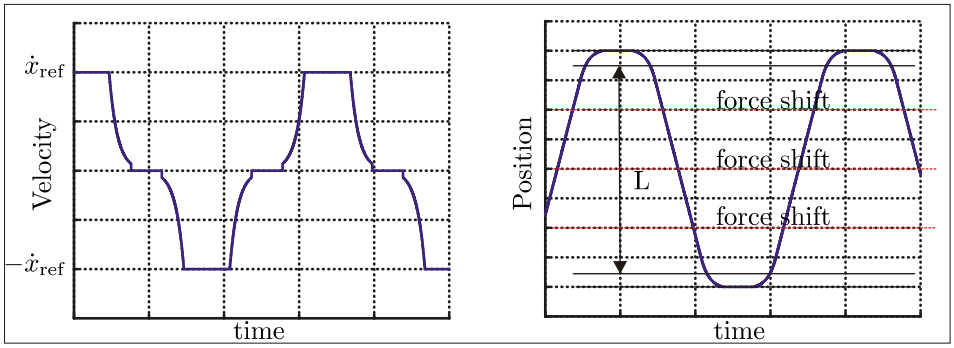

Fig. 10: Illustration of the piston movement.

Fig. 11 show measured piston position and the pressure in cylinder chamber 3 as the described test run is conducted.

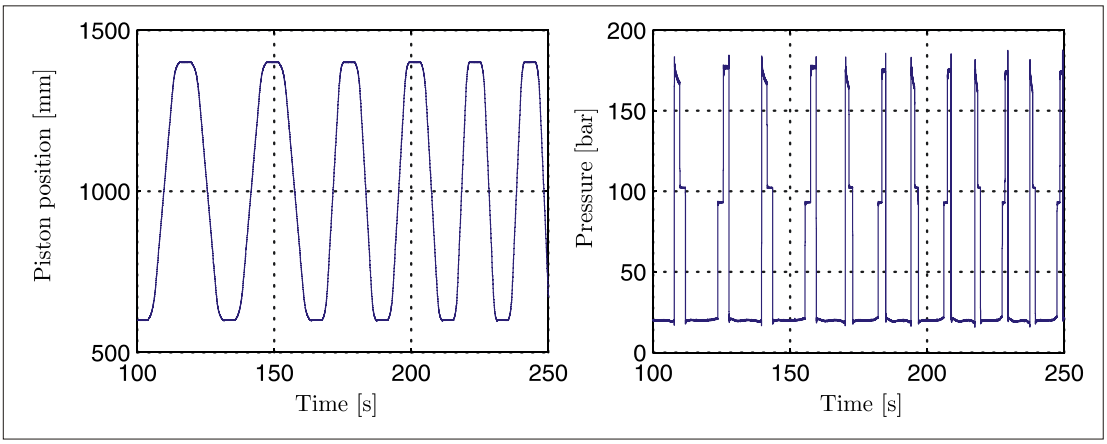

Fig. 11: Illustration of pressure shift. Left; piston position and cylinder chamber 3 pressure.

2.2.1 Implementation

The opening area algorithms are valid only in the shifting period, due to the pressure trajectories being a step wise function. Hence, some action has to be taken at the end of the shifting period to give a reasonable valve reference, which is incorporated as:

$$A_{V.max.rate}(t) = \frac{A_{V.max}}{10^{-2}} t \tag{14}$$

$$A_{V.min.rate}(t) = \frac{A_{V.max}}{15^{-2}} (t - T_d)(0 \geq (t - T_d)) \tag{15}$$

By eq. (14) and (15) a left and right limit is set in Fig. 12 respectively. The right limit as the fastest possible valve movement. And the right limit as a 15ms slew rate at a time delay T_d defined as the time needed for a passive pressure build up in the cylinder chamber.

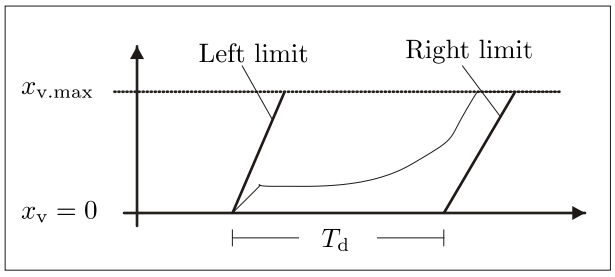

Fig. 12: Illustration of valve reference limits.

Hence,

$$A_V(t) = \min[A_V(t)\ A_{V.max.rate}(t)] \tag{16}$$

$$A_V(t) = \max[A_V(t)\ A_{V.min.rate}(t)] \tag{17}$$

$$A_{V.ref} = \min[A_V(t)\ A_{V.max}] \tag{18}$$

This implementation defines a feasible region for the valve opening area, within which the opening reference must lay. Hence, if the valve opening reference from the employed control algorithm is outside this feasible region it follows the nearest boundary.

3 RESULTS

Fig. 13 shows the valve opening reference and the resulting cylinder chamber pressure. For the current pressure shift the piston velocity is rather low, -0.05m/s and the pressure shift is from low to mid pressure, i.e. 20 to 90 bar. As seen in the upper plot the low pressure line valve are closed equally in the four cases.

Algorithms 3 and 4 are clearly preforming better with regard to pressure oscillations in this case. However, no significant difference is seen between the two algorithms 3 and 4.

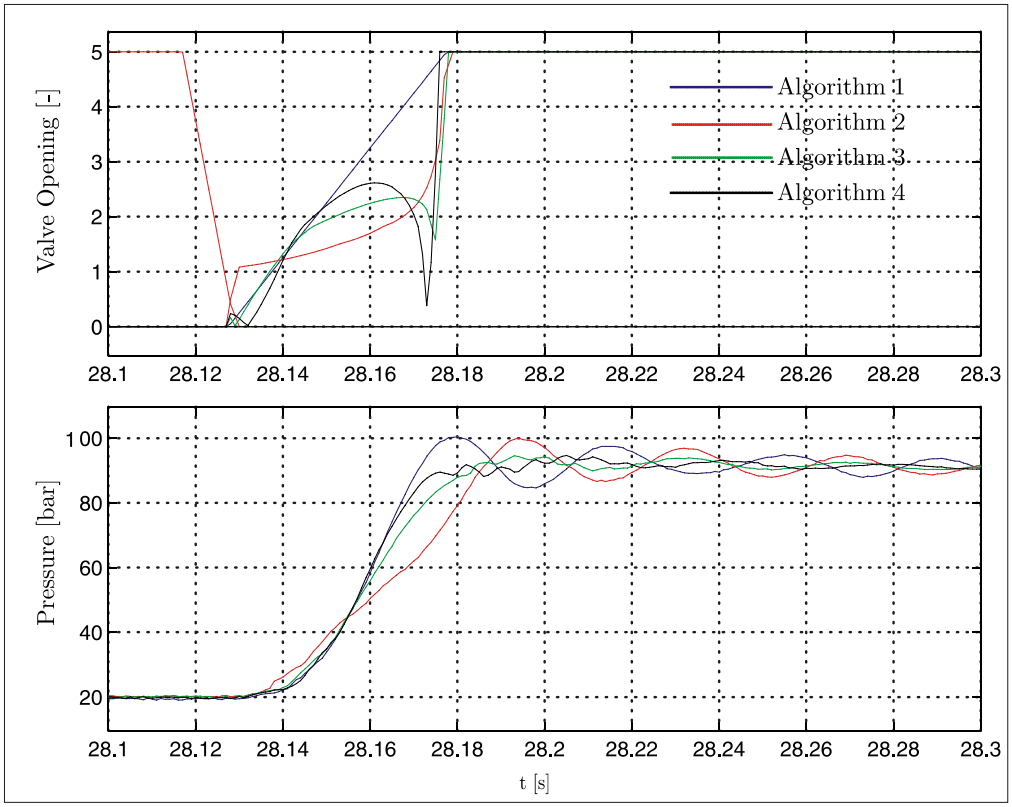

Fig. 13: Valve command and pressure measurements during pressure shift from 20 to 90 bar at $\dot{x}_c$ = -0.05m/s and x_c = 1.2m

A pressure shift from mid to high pressure is seen in Fig. 14 with similar results as for the former pressure shift from low to mid. The piston velocity is again -0.05m/s. Note, that both the two mentioned pressure shifts are performed with a chamber volume gradient supporting the given pressure shift, hence, the valve inflow is to be lower than if the piston was at rest. However, this effect is relative small due to the low velocity.

In Fig. 15 a pressure shift from high to low pressure is performed. This too is conducted with a piston velocity of -0.05m/s, however, here opposing the given pressure shift leading a larger valve flow than if at rest. For the pressure shift in Fig. 15 the algorithms 3 and 4 are again seen to impose smaller pressure oscillation than the algorithms 1 and 2.

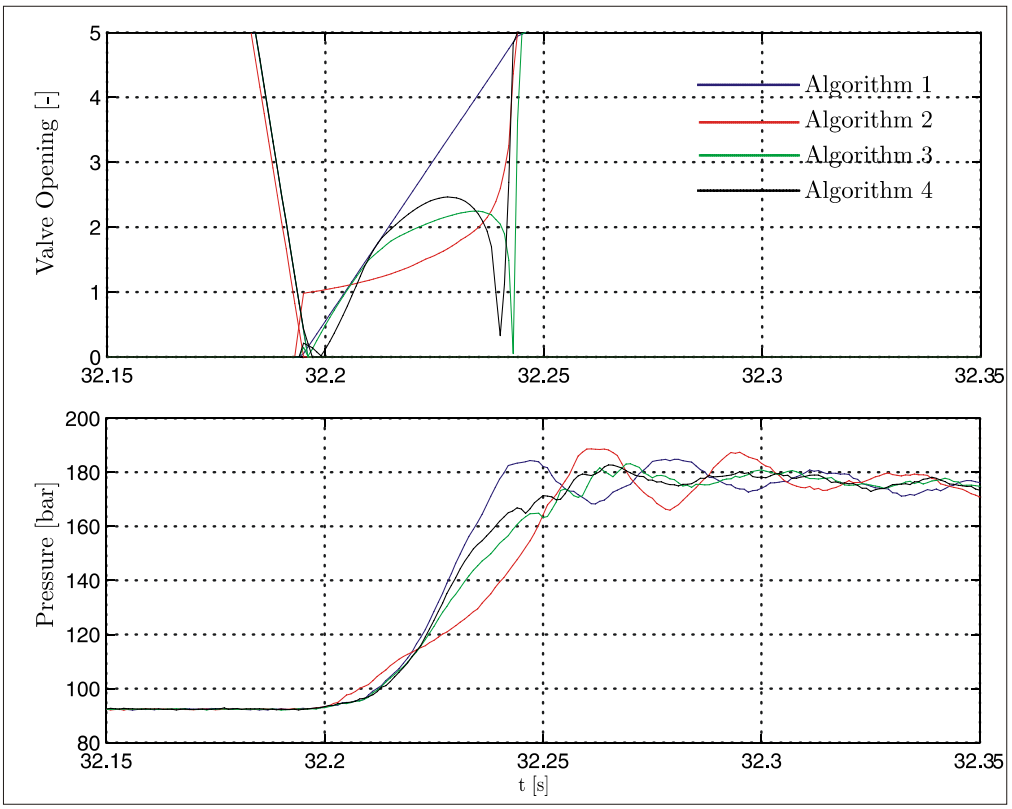

Fig. 14: Valve command and pressure measurements during pressure shift from 90 to 180 bar at $\dot{x}_c$ = -0.05m/s and x_c = 1m

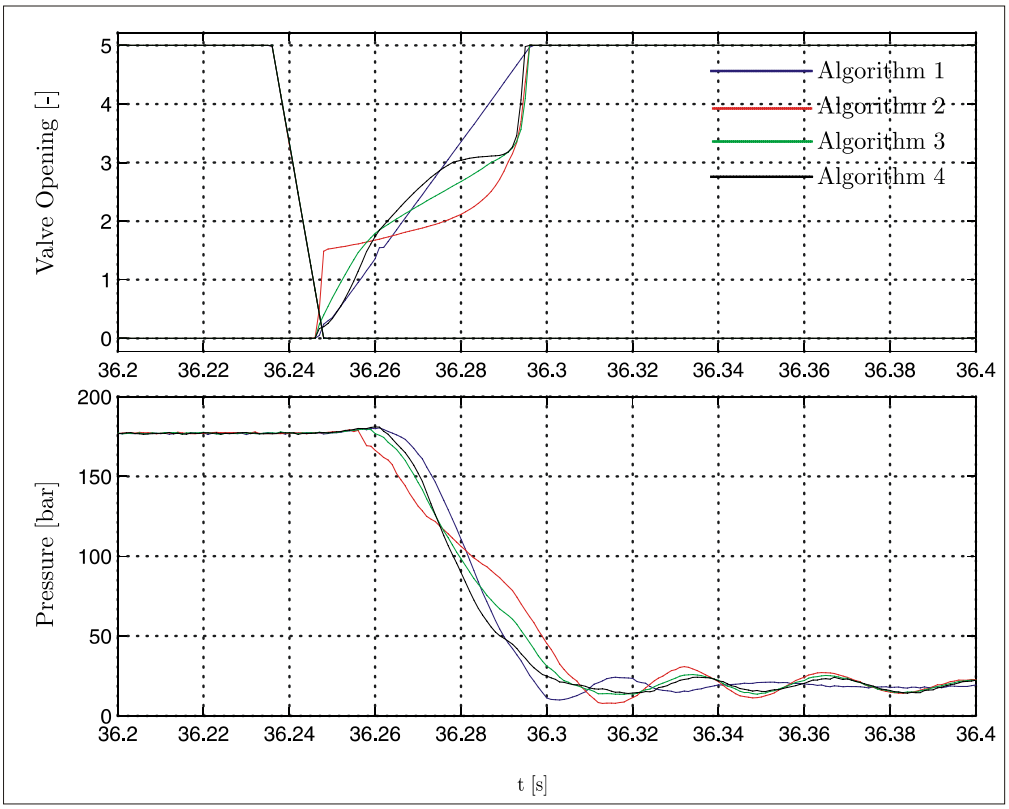

Fig. 15: Valve command and pressure measurements during pressure shift from 180 to 20 bar at $\dot{x}_c$ = -0.05m/s and x_c = 0.8m

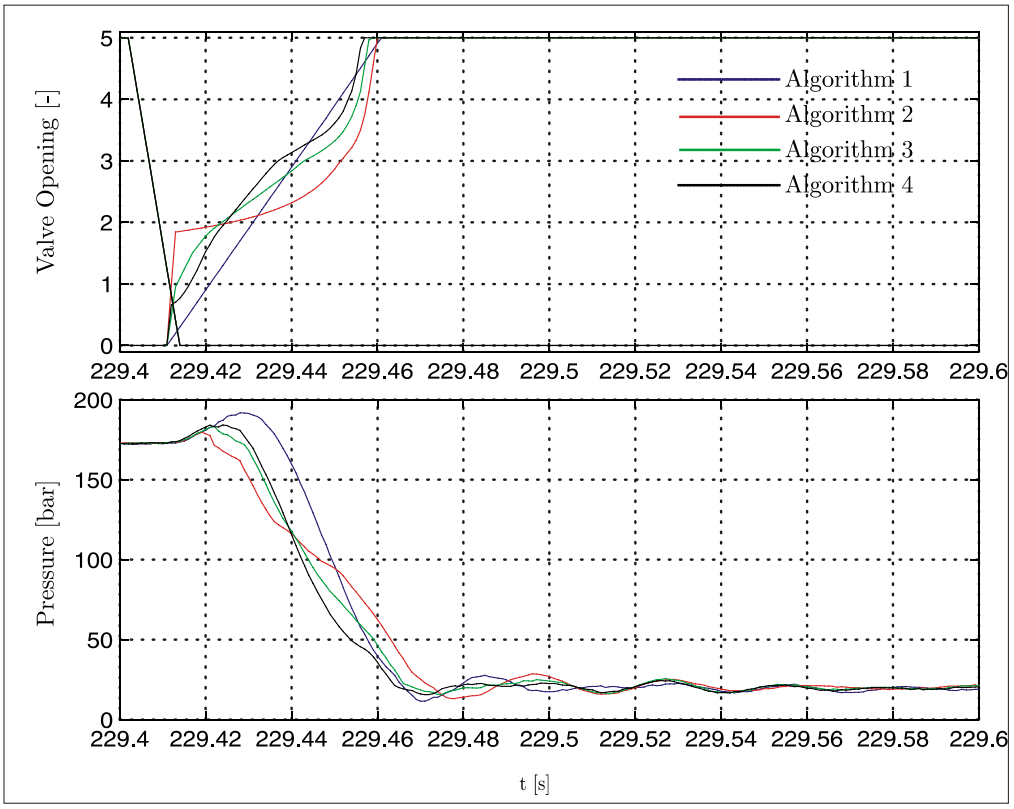

Fig. 16: Valve command and pressure measurements during pressure shift from 180 to 20 bar at $\dot{x}_c$ = -0.2m/s and x_c = 0.8m

The high to low pressure shift is in Fig. 16 shown for a piston velocity of -0.2m/s. The algorithms 3 and 4 once again show best performance. When comparing the two pressure shifts in Fig. 15 and 16, both from high to low pressure one note the difference in pressure peak before the pressure drops. This peak appears since the displacement flow is not allowed to exit the chamber during the valve closing until the new valve connection is made.

4 POWER PRODUCTION

The algorithms A2 and A3 are implemented on the test bench and tested in power production for three sea states. The average power in and output are compared as well as the efficiency. Three sea states are tested, the wave period was set to 5.5s for the three, whereas the wave hight Hm0 wrer set to [0.5 0.75 1.0]m respectively. The figure here under shows the input and output power to the left in blue and red respectively, furthermore the efficiency is given to the right.

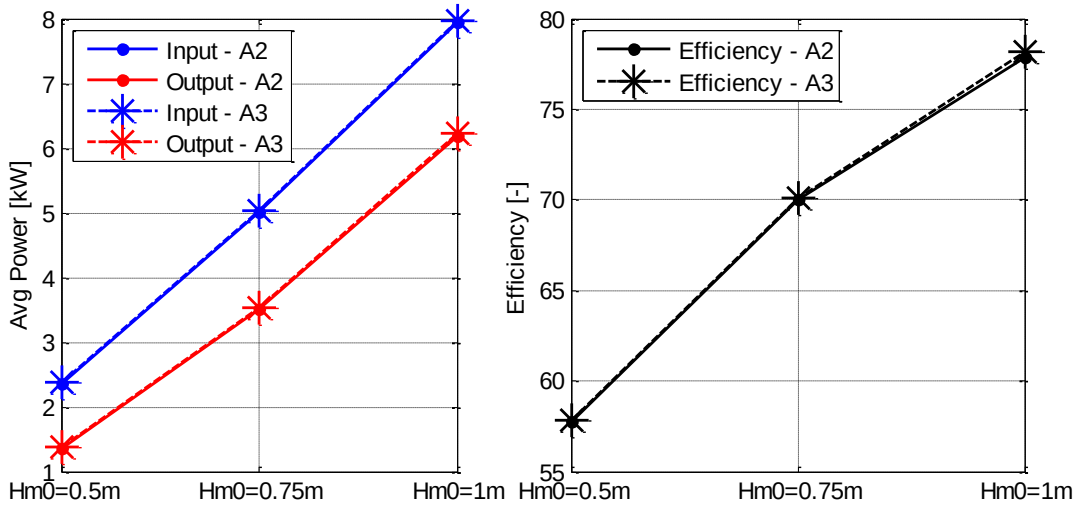

Here after a couple of screen dumps where the algorithm is given the wanted effect. One can see a significant effect when the algorithm is fitted for the chamber.

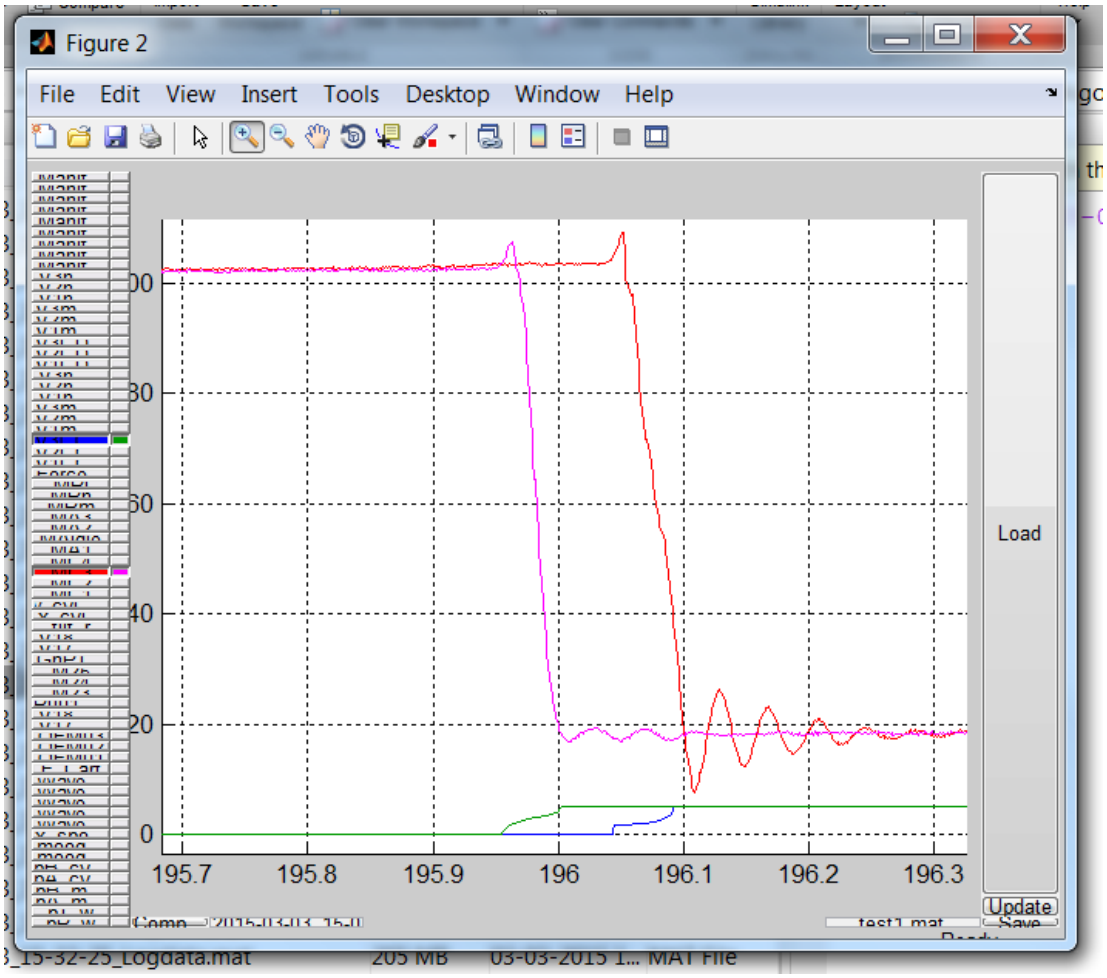

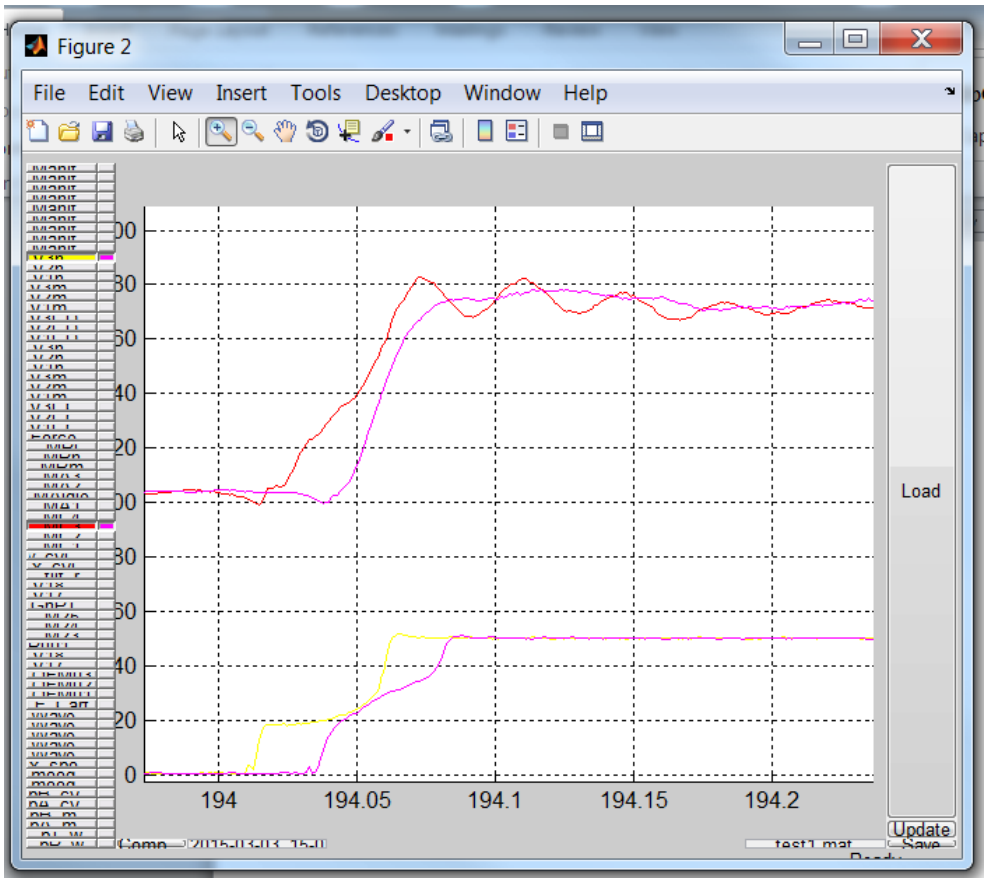

However when a situation for which the algorithm is not fitted no effect is seen.